CONCRETE LIBRARY OF JSCE NO. 25, JUNE 1995

THE FINITE ELEMENT ANALYSIS OF HEAT CONDUCTION FOR CONCRETE STRUCTURES WITH UNCERTAIN MATERIAL PROPERTIES

(Translation from Proc. of JSCE, No.496/V-24, August 1994)

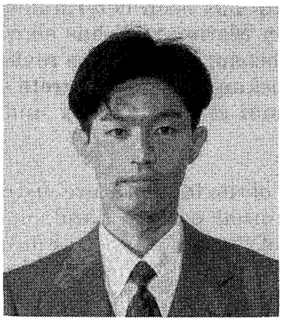

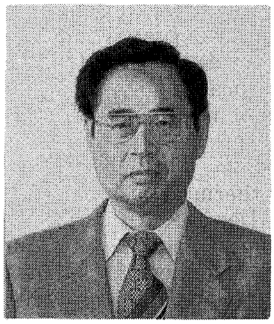

Hideaki NAKAMURA

Sumio HAMADA

An analytical procedure which deals influencing factors affecting to temperatures in the structure is herein proposed. Factor analyses were conducted against the thermal characteristics affecting to thermal analytical results by means of the method of sensitive analysis. The variances of temperature in the structure having variable thermal characteristics of concrete and environment were evaluated from the sensitivity obtained by the sensitive analysis and the approximation theory using Taylor's expansion.

Keyword: *sensitivity analysis, first-order approximation, FEM, probabilistic transient heat conduction analysis*

Hideaki Nakamura is a Research Associate in the Department of Civil Engineering at Yamaguchi University, Yamaguchi, Japan. He obtained his M.Eng. from Yamaguchi University in 1986. His research interests include thermal stress in mass concrete structure and earthquake engineering.

Sumio Hamada is a Professor in the Department of Civil Engineering at Yamaguchi University, Yamaguchi, Japan. He received his Ph.D. from the University of Alberta in Canada in 1973. His research interests include thermal stress in mass concrete structure and behavior and design of reinforced and prestressed concrete structure.

---

1. INTRODUCTION

Thermal analysis is essential in the design of massive concrete structures these days. As the scale of concrete structures becomes larger, cracks are induced by thermal stresses during curing. Experimental and analytical studies of thermal stresses in mass concrete structures have been carried out, and several procedures have been proposed for the analysis of heat conduction and thermal stress. A study of cracking probability has also been made by the committee on mass concrete thermal stresses at the Japan Concrete Institute[1], and this method is practiced in the estimation of cracking during design. The JSCE's Standard Specifications[2] for concrete were substantially reviewed as regards mass concrete structures in 1986, and an analytical method for the estimation of cracking was included. Using these methods[3,4], the cracking probability can be obtained from the relationship between thermal cracking index and cracking probability, and this relationship has been determined from the latest field surveys of mass concrete structures. A study by Morimoto[5] has shown how to carry out a more detailed evaluation of cracking, and the subcommittee for the revision of the Standard Specifications is now accumulating new data on cracking in mass concrete structures with the aim of improving the relationship between thermal cracking index and cracking probability.

Predictions of thermal cracking begin with the determination of the temperature distribution in a structure. Designs of pipe cooling systems to prevent initial cracking and pipe heating systems for road de-icing require temperature distributions of the same type. Finite element approaches to the analysis of such temperature distributions have become more widespread, as the power of workstations and personal computer develops. The analytical results, however, are considerably affected by the input data on material and environmental properties, and precise results cannot be obtained without precise data. The main thermal properties of concrete required in thermal analysis are the heat generation, thermal conductivity, heat transfer coefficient, and specific heat. These specific properties all exhibit uncertain resulting from variations in concrete materials, mix proportion, age, drying condition, atmospheric temperature, and so on. Consequently, an appropriate analytical method is now required for the analysis of temperature distribution that takes into account these uncertain physical properties.

Pipe cooling[6] and pipe heating systems[7] are now relatively common in mass concrete structures and roads in cold regions. The temperature of the heating or cooling medium in the pipe is not always stable, and engineers working in the field need to analytically determine the allowable scatter of temperature in the pipe.

Analytical results obtained in previous studies do not always agree well with experimental results, and inverse analysis[8] is often employed to obtain the appropriate specific properties of concrete. Ono[9] investigated the parameters influencing temperature rises in mass concrete. Based on his study, the parameters affecting temperature rise can be evaluated by numerical experiment. That is, the values affecting temperature rise are obtained from an analysis in which the parameters are varied by small amounts. Matsui et al[10]. presented analytical results, including the scatter of specific properties and environmental conditions, obtained in a Monte Carlo simulation. Sensitivity analysis[11] is often required in structural analysis, where the specific structural properties are vary substantially.

This study proposes a sensitivity analysis method for the thermal stresses in structures and obtains information on the influence of scatter in material and environment properties on the temperature rise in concrete structures. The analysis is based on a transient heat conduction analysis of the structure with probability parameters, and is a method which yields the mean values and scatter of temperatures in a structure. It is based on sensitivity analysis and Taylor's expansion theory. A Monte Carlo simulation can also be used to determine mean and scatter values, but enormous computational time is required for moderately precise results as compared with the this method. In order to confirm the results obtained by this new analytical method, its results are compared with those of a Monte Carlo simulation. The analysis is also applied to thick wall and slab concrete structures well as to structures requiring a pipe cooling system.

2. ANALYTICAL THEORY

2.1 FINITE ELEMENT PROCEDURE FOR TRANSIENT HEAT CONDUCTION

Sensitivity[11,12] is expressed as $\frac{\partial\phi}{\partial X_i}$ in Fig.1, where $\phi(t)$ is a nodal temperature, and X_i represents parameters such as the specific thermal properties of the material. This sensitivity gives the influence of the parameter on the nodal temperature.

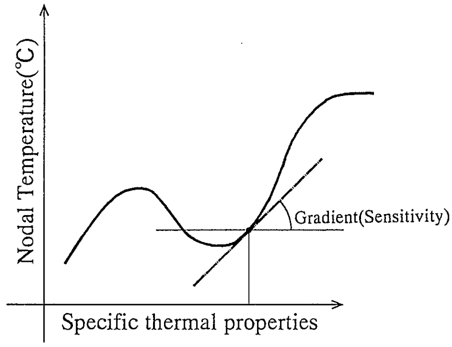

Fig.1 Sensitivity

The transient heat conduction equation discretized by the finite element method can be expressed as below[13].

$$[K]\{\phi\}+[C]\{\dot{\phi}\}=\{F\} \tag{1}$$

where $[K],\{\phi\},[C],\{\dot{\phi}\}$, and $\{F\}$ are the heat conductivity matrix, temperature vector, heat capacity matrix, vector for temperature slope with respect to time, and heat source vector, respectively.

The first derivative of the temperature vector with respect to parameter X_i is obtained by differentiating Eq.(1), yielding the following equation:

$$\frac{\partial[K]}{\partial X_i}\{\phi\}+[K]\frac{\partial\{\phi\}}{\partial X_i}+\frac{\partial[C]}{\partial X_i}\{\dot{\phi}\}+[C]\frac{\partial\{\dot{\phi}\}}{\partial X_i}=\frac{\partial\{F\}}{\partial X_i} \tag{2}$$

Rewriting Eq.(2),

$$[K]\frac{\partial\{\phi\}}{\partial X_i}+[C]\frac{\partial\{\dot{\phi}\}}{\partial X_i}=\frac{\partial\{F\}}{\partial X_i}-\frac{\partial[K]}{\partial X_i}\{\phi\}-\frac{\partial[C]}{\partial X_i}\{\dot{\phi}\} \tag{3}$$

The 2nd derivative can be determined by differentiating both sides of Eq.(3) with respect to the parameter X_j.

$$\begin{aligned}[K]\frac{\partial^2\{\phi\}}{\partial X_i\partial X_j}+[C]\frac{\partial^2\{\dot{\phi}\}}{\partial X_i\partial X_j}=&\frac{\partial^2\{F\}}{\partial X_i\partial X_j}-\frac{\partial^2[K]}{\partial X_i\partial X_j}\{\phi\}-\frac{\partial^2[C]}{\partial X_i\partial X_j}\{\dot{\phi}\}\\&-\frac{\partial[K]}{\partial X_i}\frac{\partial\{\phi\}}{\partial X_j}-\frac{\partial[K]}{\partial X_j}\frac{\partial\{\phi\}}{\partial X_i}-\frac{\partial[C]}{\partial X_i}\frac{\partial\{\dot{\phi}\}}{\partial X_j}-\frac{\partial[C]}{\partial X_j}\frac{\partial\{\dot{\phi}\}}{\partial X_i}\end{aligned} \tag{4}$$

Eqs.(1), (3), and (4) are discretized with respect to space, and not with respect to time. Derivatives with respect to time, $\{\dot{\phi}\},\frac{\partial\{\dot{\phi}\}}{\partial X_i}$ and $\frac{\partial^2\{\dot{\phi}\}}{\partial X_i\partial X_j}$, are present in Eq.(4). Discretizing these variables by the Crank-Nicolson method, the temperature at time $t+\dfrac{\Delta t}{2}$ and the derivative of temperature can be expressed respectively as

$$\left\{\phi\left(t+\frac{\Delta t}{2}\right)\right\}=\frac{1}{2}\left(\{\phi(t+\Delta t)\}+\{\phi(t)\}\right) \tag{5}$$

$$\left\{\dot{\phi}\left(t+\frac{\Delta t}{2}\right)\right\}=\frac{\{\phi(t+\Delta t)\}-\{\phi(t)\}}{\Delta t} \tag{6}$$

Substituting Eqs.(5) and (6) into Eq.(1), the following equation is obtained:

$$\left(\frac{1}{2}[K]+\frac{1}{\Delta t}[C]\right)\{\phi(t+\Delta t)\}=\left(-\frac{1}{2}[K]+\frac{1}{\Delta t}[C]\right)\{\phi(t)\}+\{F\} \tag{7}$$

The first and second sensitivities at time $t+\dfrac{\Delta t}{2}$ are expressed as

$$\frac{\partial\left\{\phi\left(t+\frac{\Delta t}{2}\right)\right\}}{\partial X_i}=\frac{1}{2}\left(\frac{\partial\{\phi(t+\Delta t)\}}{\partial X_i}+\frac{\partial\{\phi(t)\}}{\partial X_i}\right) \tag{8}$$

$$\frac{\partial\left\{\dot{\phi}\left(t+\frac{\Delta t}{2}\right)\right\}}{\partial X_i}=\frac{\dfrac{\partial\{\phi(t+\Delta t)\}}{\partial X_i}-\dfrac{\partial\{\phi(t)\}}{\partial X_i}}{\Delta t} \tag{9}$$

Substituting Eqs.(8) and (9) into Eq.(3), yields the following:

$$\begin{aligned}\left(\frac{1}{2}[K]+\frac{1}{\Delta t}[C]\right)\frac{\partial\{\phi(t+\Delta t)\}}{\partial X_i}&=\left(-\frac{1}{2}[K]+\frac{1}{\Delta t}[C]\right)\frac{\partial\{\phi(t)\}}{\partial X_i}\\&\quad+\frac{\partial\{F\}}{\partial X_i}-\frac{\partial[K]}{\partial X_i}\left\{\phi\left(t+\frac{\Delta t}{2}\right)\right\}-\frac{\partial[C]}{\partial X_i}\left\{\dot{\phi}\left(t+\frac{\Delta t}{2}\right)\right\}\end{aligned} \tag{10}$$

Similarly Eq.(4) can be written as

$$\begin{aligned}\left(\frac{1}{2}[K]+\frac{1}{\Delta t}[C]\right)\frac{\partial^2\{\phi(t+\Delta t)\}}{\partial X_i\partial X_j}&=\left(-\frac{1}{2}[K]+\frac{1}{\Delta t}[C]\right)\frac{\partial^2\{\phi(t)\}}{\partial X_i\partial X_j}\\&\quad+\frac{\partial^2\{F\}}{\partial X_i\partial X_j}-\frac{\partial^2[K]}{\partial X_i\partial X_j}\left\{\phi\left(t+\frac{\Delta t}{2}\right)\right\}-\frac{\partial^2[C]}{\partial X_i\partial X_j}\left\{\dot{\phi}\left(t+\frac{\Delta t}{2}\right)\right\}\\&\quad-\frac{\partial[K]}{\partial X_i}\frac{\partial\left\{\phi\left(t+\frac{\Delta t}{2}\right)\right\}}{\partial X_j}-\frac{\partial[K]}{\partial X_j}\frac{\partial\left\{\phi\left(t+\frac{\Delta t}{2}\right)\right\}}{\partial X_i}\end{aligned}$$

$$-\frac{\partial[C]}{\partial X_i}\frac{\partial\left\{\dot{\phi}\left(t+\frac{\Delta t}{2}\right)\right\}}{\partial X_j}-\frac{\partial[C]}{\partial X_j}\frac{\partial\left\{\dot{\phi}\left(t+\frac{\Delta t}{2}\right)\right\}}{\partial X_i} \tag{11}$$

$\phi\left(t+\frac{\Delta t}{2}\right)$ and $\dot{\phi}\left(t+\frac{\Delta t}{2}\right)$ on the right-hand side of Eq.(10) can be determined by taking values from Eq.(7). $\frac{\partial\left\{\phi\left(t+\frac{\Delta t}{2}\right)\right\}}{\partial X_i}$ and $\frac{\partial\left\{\dot{\phi}\left(t+\frac{\Delta t}{2}\right)\right\}}{\partial X_i}$ on the right-hand side of Eq.(11) are also determined in the same manner from Eqs.(11) and (10) by substituting the values obtained from Eq.(10) into these equations.

2.2 APPROXIMATE THEORY BASED ON TAYLOR'S EXPANSION[14]

The nodal temperatures in a structure with scattered specific properties can be determined using the sensitivities evaluated in the previous section. Since each nodal temperature in the structure is a function of probability variables $X_1, X_2, \cdots\cdots, X_n$, it is given by

$$\phi = g(X_1, X_2, \cdots, X_n) \tag{12}$$

The following equation is obtained by Taylor's expansion near to the expectation $\overline{X} = \{\overline{X}_1, \overline{X}_2, \cdots, \overline{X}_n\}$, as follows,

$$\phi = g(\overline{X}_1, \overline{X}_2, \cdots, \overline{X}_n) + \sum_{i=1}^{n}\left(\frac{\partial g}{\partial X_i}\right)_{\overline{X}}(X_i - \overline{X}_i) + \cdots\cdots$$
$$+\frac{1}{2}\sum_{i=1}^{n}\sum_{j=1}^{n}\left(\frac{\partial^2 g}{\partial X_i \partial X_j}\right)_{\overline{X}}(X_i - \overline{X}_i)(X_j - \overline{X}_j) + \cdots\cdots \tag{13}$$

where $(\ \cdot\ )_{\overline{X}}$ implies derivatives with respect to $(\overline{X}_1, \overline{X}_2, \cdots, \overline{X}_n)$.
Neglecting higher orders than the second order in Eq.(13), the expectation $E[\phi]$ and variance $Var[\phi]$ are represented respectively by

$$E[\phi] = g[\overline{X}_1, \overline{X}_2, \cdots, \overline{X}_n] \tag{14}$$

and

$$Var[\phi] = \sum_{i=1}^{n}\sum_{j=1}^{n}\left(\frac{\partial\phi}{\partial X_i}\right)_{\overline{X}}\left(\frac{\partial\phi}{\partial X_j}\right)_{\overline{X}} Cov[X_i, X_j] \tag{15}$$

$Cov[X_i, X_j]$ implies the second moment with respect to the expectation and is nominated as the covariance. This procedure is called the first-order approximation.

Neglecting higher orders than the third order on the right-hand side of Eq.(13), the second-order approximation can be obtained as

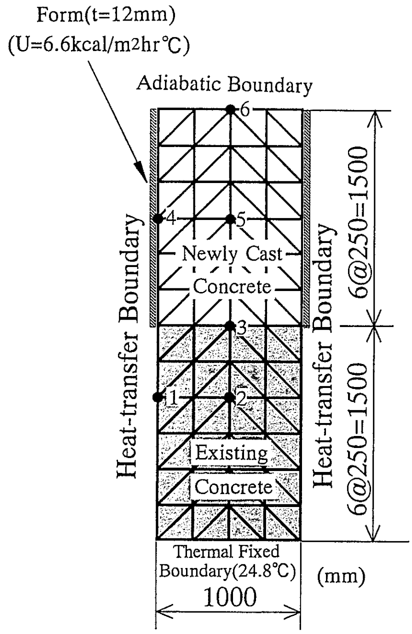

Fig.2 Finite Elemt Mesh and Boundary Conditions

Table 1 The Properties for Analysis

Specific Heat(C_c) kcal/kg•℃ (J/kg•℃)	0.302 (1264)
Thermal Conductivity(λ_c) kcal/m•hr•℃ (W/m•℃)	2.424 (2.819)
Heat-transfer Coefficient(h_c) kcal/m^2•hr•℃ (W/m^2•℃)	12.0 (14.0)
Density (ρ_c) kg/m^3	2300
Initial Temperature ℃	29.8
Ambient Temperature(T_{out}) ℃	24.8
Adiabatic Heat Generation $T_{ad}=K(1-e^{-\alpha t})$	K = 48.5℃ $\alpha=1.426$

Table 2 Values Based on the SI System

Specific Heat	1kcal/kg•℃ = 4.186×10^{3}J/kg•℃
Thermal Conductivity	1kcal/m•hr•℃ = 1.163W/m•℃
Heat-transfer Coefficient	1kcal/m^2•hr•℃ = 1.163W/m^2•℃

$$E[\phi]=\phi(\bar{X}_1,\bar{X}_2,\cdots,\bar{X}_n)+\frac{1}{2}\sum_{i=1}^{n}\sum_{j=1}^{n}\left(\frac{\partial^2\phi}{\partial X_i\partial X_j}\right)_{\bar{X}}Cov[X_i,X_j] \tag{16}$$

$$\begin{aligned}Var[\phi]=&\sum_{i=1}^{n}\sum_{j=1}^{n}\left(\frac{\partial\phi}{\partial X_i}\right)_{\bar{X}}\left(\frac{\partial\phi}{\partial X_j}\right)_{\bar{X}}Cov[X_i,X_j]+\sum_{i=1}^{n}\sum_{j=1}^{n}\sum_{k=1}^{n}\left(\frac{\partial\phi}{\partial X_i}\right)_{\bar{X}}\left(\frac{\partial^2\phi}{\partial X_i\partial X_j}\right)_{\bar{X}}\\&\times E\left[(X_i-\bar{X}_i)(X_j-\bar{X}_j)(X_k-\bar{X}_k)\right]+\frac{1}{4}\sum_{i=1}^{n}\sum_{j=1}^{n}\sum_{k=1}^{n}\sum_{l=1}^{n}\left\{\left(\frac{\partial^2\phi}{\partial X_i\partial X_j}\right)_{\bar{X}}\left(\frac{\partial^2\phi}{\partial X_k\partial X_l}\right)_{\bar{X}}\right.\\&\left.\times\left(E\left[(X_i-\bar{X}_i)(X_j-\bar{X}_j)(X_k-\bar{X}_k)(X_l-\bar{X}_l)\right]\right)-Cov[X_i,X_j]Cov[X_k,X_l]\right\}\end{aligned} \tag{17}$$

The mean and expectation values can be determined by substituting the sensitivities obtained from Eqs.(1) and (11) into Eqs.(14) and (15) or Eqs.(16) and (17).

3. NUMERICAL EXAMPLES OF SENSITIVITY ANALYSIS

Analytical temperature results cannot be determined to great accuracy without the exact values of specific properties, yet these specific properties are presumably scattered in the case of concrete. The specific properties of concrete needed in thermal analysis are heat generation, thermal conduction, heat transfer coefficient, and specific heat, and these have uncertainties relating to age, mix proportion, drying conditions, and temperature. The other causes of scatter are the environment surrounding the concrete, and differences in testing methods. In this chapter, we indicate how to evaluate the factors influencing concrete temperature from the sensitivity analysis.

3.1 TEMPERATURE ANALYSIS

3.1.1 Analytical Model and Analytical conditions

The wall structure described in reference [1] is used as an example in this analysis. The specific heat properties which influence temperature in concrete may be regarded as the coefficients of adiabatic heat generation (K, α), the specific heat (C_c), the concrete density (ρ_c), the thermal conductivity (λ_c), the heat transfer coefficient (h_c), the coefficient of overall heat transmission of form (U), and the ambient temperature (T_{out}). Their influence on nodal temperature can be determined by evaluating the sensitivities $\frac{\partial\{\phi\}}{\partial K}$, $\frac{\partial\{\phi\}}{\partial \alpha}$, $\frac{\partial\{\phi\}}{\partial C_c}$, $\frac{\partial\{\phi\}}{\partial \rho_c}$, $\frac{\partial\{\phi\}}{\partial \lambda_c}$, $\frac{\partial\{\phi\}}{\partial h_c}$, $\frac{\partial\{\phi\}}{\partial U}$, and $\frac{\partial\{\phi\}}{\partial T_{out}}$. Figure 2 illustrates the finite element mesh and boundary conditions. Table 1 gives data for the analysis of the wall structure. The adiabatic heat generation in this analysis is assumed to be

$$T_{ad} = K\left(1 - e^{-\alpha t}\right) = K\left(1 - e^{-\frac{\alpha}{24}t'}\right) \tag{18}$$

where T_{ad} is rise in temperature at age t (℃), K and α are coefficients, and t and t' are ages of concrete in day and hour, respectively. Differentiating Eq.(18) with respect to t' gives the adiabatic rise in temperature, as follows.

$$\frac{dT_{ad}(t')}{dt'} = \frac{K\alpha}{24} e^{-\frac{\alpha}{24}t'} \tag{19}$$

Consequently, the heat generated per unit time and unit volume is represented by

$$\dot{Q} = \rho_c C_c \frac{K\alpha}{24} e^{-\frac{\alpha}{24}t'} \tag{20}$$

which is equivalent to the internal heat generated in an element of the concrete shown in Fig.2. We evaluate sensitivity at six nodes at intervals of one hour.

3.1.2 Results of Sensitivity Analysis

The temperature histories for the six nodes in the structure marked in Fig.2 are illustrated in Fig.3. The sensitivities of coefficients K and α, thermal conductivity, heat transmission rate, and atmospheric temperatures are also illustrated in Figs.4 to 9, respectively. The ordinate in these figures represents sensitivity, which reflects nodal temperature change due to a unit change in each specific property from the standard value given in Table 1. The temperature rises with increasing sensitivity, and falls as it decreases. The unit of the ordinate is temperature divided by the unit of the specific coefficient. Values based on the SI system are also given in the table. Figure 4 points out that sensitivity varies with location and time. The values of sensitivity are larger for newly cast concrete, and the peak value is reached after approximately one day. On the other hand, the sensitivity values are fairly small for existing concrete, which implies that the heat generated in newly cast concrete influences sensitivity. Figure 5 shows that the coefficient α influences the temperature more at an early stage compared with the other coefficients. According to Fig.6, the temperature is sensitive to thermal conductivity in both the positive and negative directions, depending on whether the concrete is newly cast or old. The sensitivity to heat transfer coefficient, as shown in Fig.7, decreases with passing time. Since the difference between atmospheric temperature and the temperature in a concrete structure is small, the coefficient does not affect nodal temperatures

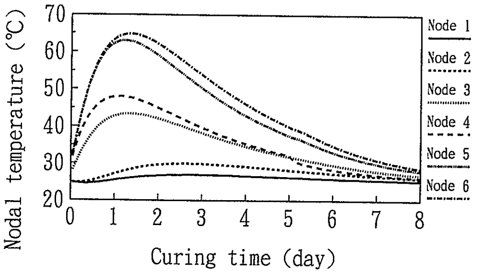

Fig.3 The Temperature Histories

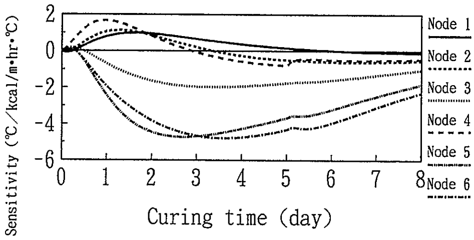

Fig.6 The Sensitivity Histories of Thermal Conductivity

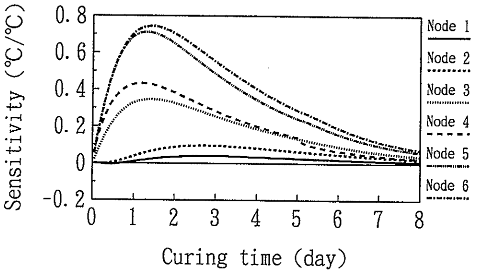

Fig.4 The Sensitivity Histories of K

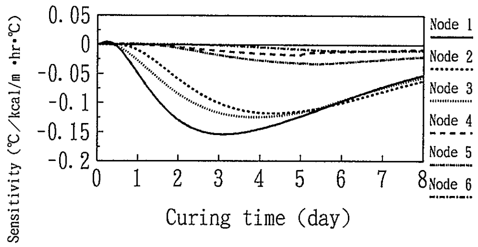

Fig.7 The Sensitivity Histories of Heat Transfer Coefficient

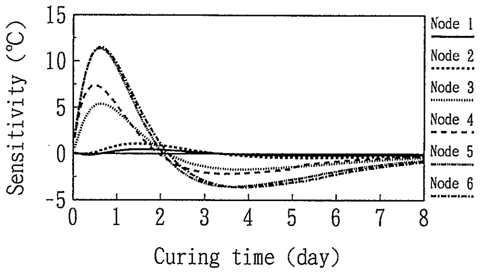

Fig.5 The Sensitivity Histories of α

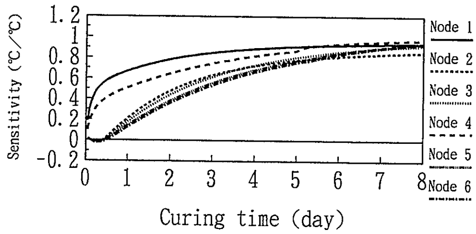

Fig.8 The Sensitivity Histories of Ambient Temperature

at an early stage. As time advances, sensitivity to the coefficient becomes greater due to the large difference in temperature. Negative values imply a heat transfer from the concrete to the atmosphere. The sensitivity to atmospheric temperature becomes greater as time advances, asymptotically approaching a constant value of unity, as indicated in Fig.8.

3.1.3 Factors Influencing Nodal Temperature

In order to obtain information on the degree of influence of specific heat properties and environmental properties on the temperature, the change in temperature at node 6 are shown in Fig.9 for the case where each parameter varies by

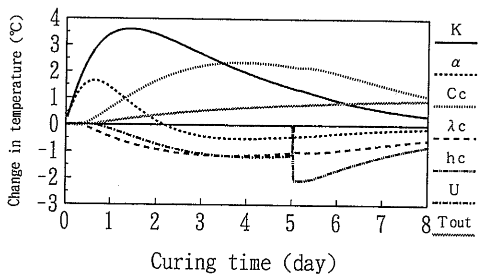

Fig.9 The Change in Temperature at node 6

Table 3 The Properties for the Analysis

	Concrete	Rock
Specific Heat kcal/kg•℃(J/kg•℃)	0.21 (871)	0.38 (1591)
Thermal Conductivity kcal/m•hr•℃(W/m•℃)	1.9 (2.21)	1.1 (1.28)
Heat-transfer Coefficient kcal/m^2•hr•℃(W/m^2•℃)	10.0 (11.63)	10.0 (11.63)
Density kg/m^3	2300	1800
Initial Temperature ℃	20.0	20.0
Ambient Temperature ℃	20.0	
Adiabatic Heat Generation	K=40.0℃ α=0.755	

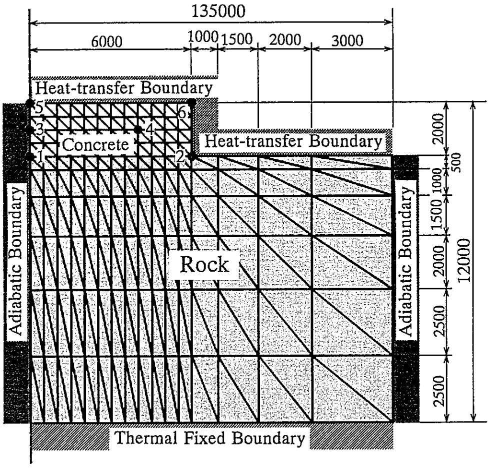

Fig.10 Finite Element Mesh and Boundary Conditions

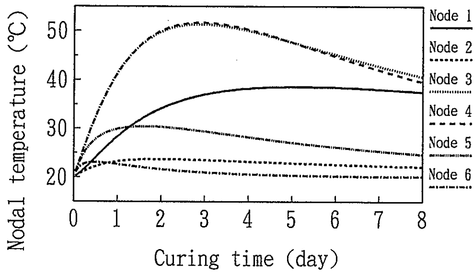

Fig.11 The Temperature histories

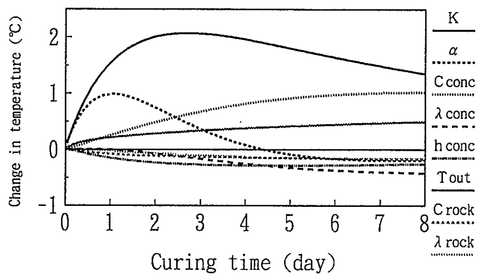

Fig.12 The change in temperature at node 4

10% from the standard value. Since 10% of atmospheric temperature is meaningless (It would be 2℃ at 20℃ and 0℃ at 0℃), the parameter for the environment is varied by 1℃.

Figure 9 illustrates that the specific adiabatic rise in temperature, K, and the specific heat affect the temperature in the concrete. Parameter α has an influence at an early stage. The influence due to heat transfer coefficient is small within the first five days because of the forms, which are removed at the 5th day. A sudden change in sensitivity to heat transfer coefficient occurs at the 5th day for the same reason. The computation results indicate that the influence of atmospheric temperature is not insignificant and a difference in the atmospheric temperature between that assumed in the analysis and that of the actual curing period may affect the concrete temperature considerably. Assuming that these various sensitivities do not correlate, the temperature in structures with various different properties can be easily determined by superimposition of the sensitivities in Fig.9 multiplied by the differences in the parameters.

3.2 THERMAL ANALYSIS OF CIRCULAR SLABS

3.2.1 Analytical Model and Properties

The second analytical example is a circular slab 6m in diameter and 2m in thickness cast on rock. An axis-symmetric finite element model is employed in the analysis, as shown in Fig.10. Table 3 provides the properties for the analysis.

3.2.2 Factors Affecting Nodal Temperature

Figure 11 shows the temperature histories of the six nodes marked in Fig.10. Figure 12 shows the temperature differences at node 4 for a 10% change in each parameter.

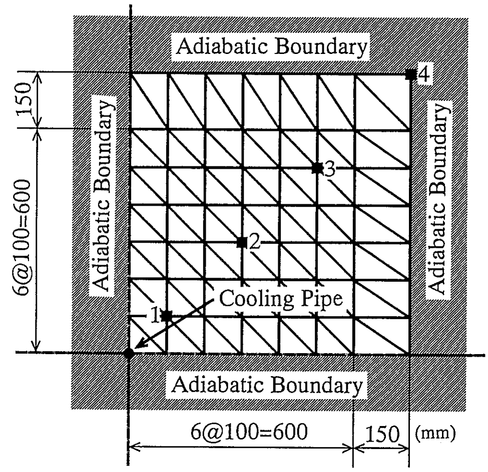

Fig.13 Finite Element Mesh and Boundary Conditions

Table 4 Analytical Conditions

Specific Heat kcal/kg•℃ (J/kg•℃)	0.21 (879)
Thermal Conductivity kcal/m•hr•℃ (W/m•℃)	2.00 (2.33)
Heat-transfer Coefficient kcal/m^2•hr•℃ (W/m^2•℃)	10.0 (11.63)
Density kg/m^3	2300
Initial Temperature ℃	30.0
Adiabatic Heat Generation	K =40.0℃ α =0.889
Heat-transfer Coefficient of Pipe kcal/m^2•hr•℃(W/m^2•℃)	233 (271)
Cooling Water Temperature ℃	10.0
Pipe Diameter m	0.025

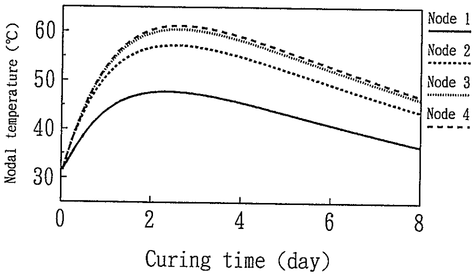

Fig.14 The Temperature Histories

A similar tendency to that in the wall structure is seen, where are parameter, K, and the specific heat influence the change in nodal temperature for equal variations in specific heat properties. The coefficient α influences the initial nodal temperature during adiabatic temperature rise. The specific heat properties of the rock base do not influence nodal temperatures. This study demonstrates that fairly precise data for K and α are required in order to obtain accurate analytical results.

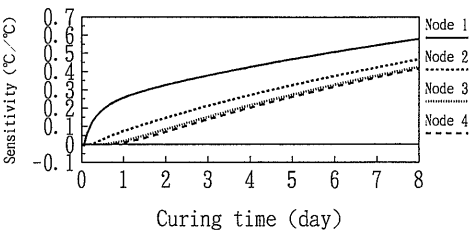

Fig.15 The Sensitivity Histories of Cooling Water Temperature

3.3 THERMAL ANALYSIS OF PIPE COOLING

Pipe cooling systems are often adopted in mass concrete structures. In such cased, the pipe size, pipe spacing, flow rate, water temperature, flow time, and so on must be known to suitable accuracy. Accordingly, the factors influencing concrete temperature are investigated by employing the sensitivity analysis procedure on an existing structure.

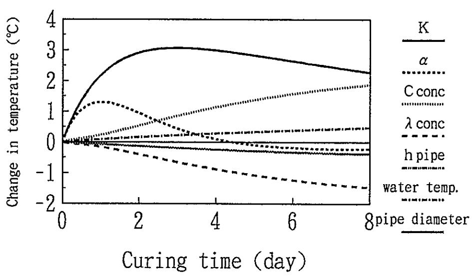

Fig.16 The Change in Temperature

3.3.1 Analytical Model

Analysis is carried out on a concrete structure with cooling pipes, part of which is shown in Fig.13, under the conditions given in Table 4. A pipe element is assumed to be a heat transfer boundary with a temperature equal to that of the cooling water. The heat transfer coefficient between the cooling pipe and cooling water, at a velocity of 40cm/s, is determined using the equation proposed by Tanabe[6]. The analysis cares eight days with an interval of 0.1 hour for first 10 hours and an interval of one hour thereafter.

3.3.2 Analytical Results

Temperature histories for the four nodes shown in Fig.13 are obtained as exhibited in Fig.14. Figure 15 indicates that the sensitivity to cooling water is higher as the temperature rises. The sensitivity increases linearly after the 2nd day. This implies that the influence of cooling by water exceeds that of the heat of hydration on the 2nd day. Figure 16 shows the mean variance of the four node temperatures at for 10% change in all parameters, except cooling water temperature, which changes by 1℃. The coefficients of adiabatic temperature rise, K and α, also influence the nodal temperatures. The specific heat and heat conductivity have a considerable influence on the temperature. The influence of heat transfer coefficient is almost the same as that of pipe diameter, which implies that increasing the pipe diameter would have an effect equal to that of reducing the heat transfer coefficient.

4. THERMAL ANALYSIS OF CONCRETE STRUCTURES WITH UNCERTAIN SPECIFIC HEAT PROPERTIES

A thermal analysis was conducted to determine the scatter in temperature based on the sensitivities and approximate Taylor expansion, when each specific heat property and environmental property varies. The Monte Carlo simulation is well known in sensitivity analysis, but the method requires numerous transient thermal analyses in order to obtain accurate and reliable results. Here, we carryout a sensitivity analysis on a wall structure with seven scattered parameters, and the results are compared with the results obtained by a Monte Carlo simulation. Taking the eight stochastic variables used in a Monte Carlo simulation as normal stochastic variables, transient thermal analysis was conducted for 5,000 cases of each stochastic variable. The sampling method proposed in reference [15] is employed in evaluating correlative stochastic variables. Table 1 provides the specific thermal properties adopted as fundamental data. The analysis is conducted based on the data given in Table 1, assuming that each specific property follows a normal distribution function. The expected value and variance of nodal temperatures with the eight stochastic variables are determined from the following equations.

$$E[\phi] = g\left(\bar{K},\bar{\alpha},\bar{C}_c,\bar{\rho}_c,\bar{\lambda}_c,\bar{h}_c,\bar{U},\bar{T}_{out}\right) \tag{21}$$

$$Var[\phi] = \left(\frac{\partial g}{\partial K}\right)^2 Var[K] + \left(\frac{\partial g}{\partial K}\right)\left(\frac{\partial g}{\partial \alpha}\right) Cov[K,\alpha] + \cdots\cdots$$
$$\cdots\cdots + \left(\frac{\partial g}{\partial T_{out}}\right)\left(\frac{\partial g}{\partial U}\right) Cov[T_{out},U] + \left(\frac{\partial g}{\partial T_{out}}\right)^2 Var[T_{out}] \tag{22}$$

where $g(\cdot)$, $Var[X_i]$, and $Cov[X_i]$ are functions for the evaluation of nodal temperature, variance of a specific thermal property, and covariance of the mutual specific thermal properties, respectively.

The variance and covariance of mutual specific thermal properties can be determined from the following equations.

$$Var[X_i] = \left(\nu_{x_i} \cdot E[X_i]\right)^2 \tag{24}$$

$$\mu_{x_i x_j} = \frac{Cov[X_i, X_j]}{\sqrt{Var[X_i]}\sqrt{Var[X_j]}} \tag{25}$$

where, ν_{x_i} and $\mu_{x_i x_j}$ are the coefficients of variation of the specific thermal properties, X_i, and coefficients of correlation, respectively. The expected value and variance to a second-order approximation can be evaluated from Eqs. (16) and (17), and the third-order moment is 0 and

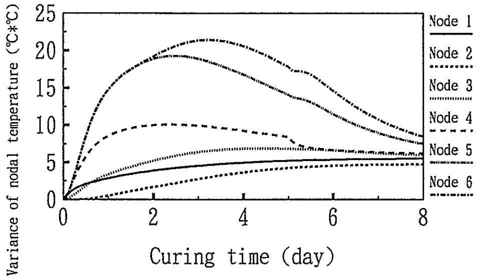

Fig.17 The Variance of Nodal Temperature

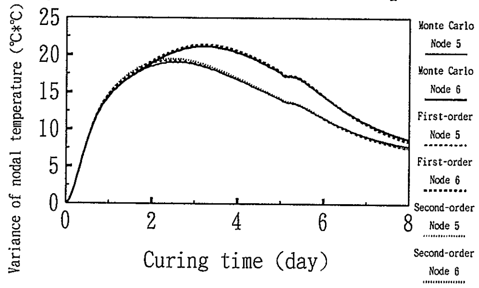

Fig.18 The Scattering History at Node 5 and 6

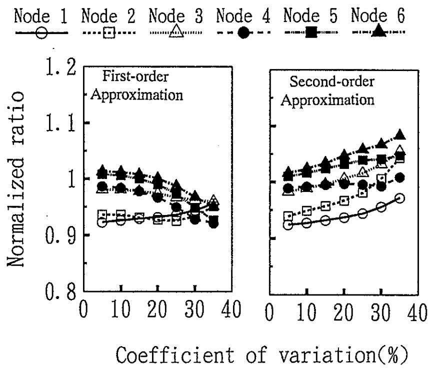

Fig.19 The Accuracy of Analysis

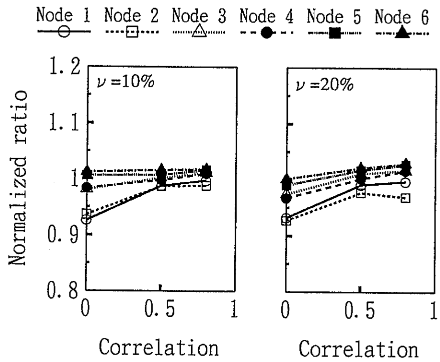

Fig.20 The Accuracy of Analysis

the fourth can be determined as a function of the second-order moment[14].

4.1 VARIANCE OF NODAL TEMPERATURE

Figure 17 shows the variance of nodal temperature obtained from the first-order approximation method, when the eight specific thermal properties have a coefficient of variation of 10%. Figure 18 shows the scattering history at nodes 5 and 6 evaluated using the Monte Carlo simulation, the first-order approximation method, and second-order approximation method. The period of the maximum scatter is the 2nd to 4th days, and is longer than the time at the maximum temperature. This is due to the influence of properties with the later maximum sensitivity shown in Figs.4 to 8. Figure 18 shows that the scatter in nodal temperature evaluated by the first-order and second-order approximation methods are close to those evaluated by the Monte Carlo simulation.

4.2 DIFFERENCE IN ANALYTICAL RESULTS BETWEEN THE NEW METHOD AND THE MONTE CARLO METHOD

In order to investigate the applicability of the new method to sensitivity analysis, its results are compared with those of a Monte Carlo simulation. The normalized ratio of these results to the Monte Carlo results is employed for this purpose. This normalization is given as

$$e = \sqrt{\frac{\sum_{i=1}^{n}(T_{si} / T_{mi})}{n}} \tag{25}$$

where n, T_{si}, and T_{mi} are the number of computations, the scatter in the results, and the scatter in Monte Carlo results.

Figure 19 depicts the normalized values for first-order and second-order approximations, when the correlation is zero. In the case of the first-order approximation, it gradually decreases with increasing coefficient of variation, whereas for the second-order approximation it increases with increasing coefficient of variation. Since these normalized values are both fairly close to unity, the first-order approximation method is sufficient for sensitivity analysis. Figure 20 shows the normalized value when each parameter has a correlation, which provides better accuracy.

5. CONCLUSION

This study describes a procedure for obtaining the quantitative influence of specific thermal properties and environmental properties on concrete temperature due to hydration heat, as well as a procedure for determining the scatter of temperature in a concrete structure when there is scatter in the specific thermal properties and environmental properties. The analytical procedure was applied to wall and footing structure and a pipe cooling structure. The following conclusions have been reached:

(1) This method of sensitivity analysis provides a quantitative measure of the influence of random specific properties on concrete temperature.

(2) Results obtained with this analysis agree well with the results of a Monte Carlo simulation within the range of a 35% coefficient of variation.

(3) Both first- and second-order approximation methods give similar results for the scatter, implying that a first-order approximation method is adequate for determining the scatter.

(4) This new analysis method offers fairly accurate results for specific properties that correlate with each other.

Acknowledgment

The authors express their appreciation to the members of the Subcommittee on Mass Concrete (Chairman: Kokubu; secretary general: Ono) in the concrete Standard Specifications Committee, who gave valuable suggestions.

References

[1] JCI: “Recommendation for the Control of Cracking of Mass Concrete,” JCI, 1986
[2] JSCE: “Concrete Standard Specifications,” JSCE, 1991
[3] H. Morimoto and W. Koyanagi: “Study on the Estimation of Thermal Cracking in Concrete Structures ,” Proc. of the 39th Annual Conference of the JSCE, 5, pp.291-292, 1984
[4] H. Morimoto and W. Koyanagi: “Study on the Estimation of Thermal Cracking in Concrete Structures,” Proc. of JCI, Vol.8, pp.53-56, 1986
[5] H. Morimoto and W. Koyanagi: “Study on the Estimation of Thermal Cracking in Concrete Structures,” Proc. of JSCE, No.390/V-8, pp.67-75, 1988
[6] T. Tanabe, H. Yamakawa and A. Watanabe: “Determination of Convection Coefficient at Cooling Pipe Surface and Analysis of Cooling Effect,” Proc. of JSCE, No.343, pp.171-179, 1984
[7] S. Tanaka, H. Nakamura and S. Hamada: “Snow-melting and Antifreeze System for Prevention of Auto Accidents on Slippery Bridge Decks,” Proc. of JCI, Vol.15, No.1, pp.1201-1206, 1993
[8] H. Chikahisa, J. Tsuzaki, Y. Arai and S. Sakurai: “Estimation of Heat Transfer Coefficients of Mass Concrete Structures by Means of Back Analysis,” Proc. of JSCE, No.451/V-17, pp.39-47, 1992
[9] S. Ono: “Studies on Various Factors Affecting the Temperature Rise of Mass Concrete and Proposal of a Calculation Method for the Temperature Rise,” Proc. of JSCE, No.348/V-1, pp.123-132, 1984
[10] K. Matsui, N. Nishida, Y. Dobashi and K. Ushioda: “Thermal Stress in Massive Concrete

under Uncertain Parameters," Proc. of JCI, Vol.15, No.1, pp.1143-1148, 1993
[11] H. Otsubo, el al.: "Sensitive Analysis (No.1)," Journal of the Japan Marine Engineers, No.714, pp.23-31, 1988
[12] H. Otsubo, el al.: "Sensitive Analysis (No.2)," Journal of the Japan Marine Engineers, No.716, pp.16-22, 1989
[13] G. Yagawa: "Finite Element Analysis in Fluid Dynamics and Heat Transfer," Baifukan, 1983
[14] S. Nakagiri and T. Hisada: "Stochastic Finite Element Method," Baifukan, 1985
[15] M. Hoshiya and K. Ishii: "Reliability Design for Structures," Kajima Syuppan-kai, pp.88-90, 1986